AKADÉMIAI KIADÓ

Pollack Periodica • An International Journal for Engineering and Information Sciences

17 (2022) 3, 65–70

DOI: 10.1556/606.2022.00603

ORIGINAL RESEARCH PAPER

Practical extension of ideal gas model for propane explosion simulation

Viktoria Mikaczo*, Zoltan Simenfalvi and Gabor L. Szepesi

Institute of Energy Engineering and Chemical Machinery, Faculty of Mechanical Engineering and Informatics, University of Miskolc, Miskolc-Egyetemváros, Hungary

Received: January 17, 2022 • Revised manuscript received: May 1, 2022 • Accepted: May 13, 2022
Published online: August 17, 2022

ABSTRACT

To estimate and model explosion pressure rise in closed volumes, industrial applications require a simple method. Ideal gas model is capable to assume pressure rise values to 10% above to initial pressure. However, most of the explosion venting devices opens higher than this pressure range.

Extension of ideal gas model was carried out in this paper. Authors made some experimental studies in 20 L explosion sphere at ambient temperature and atmospheric initial pressure, with propane-air mixtures at different concentrations between 2.8 and 6.3 vol%. They measured pressure values inside the chamber during explosion and recorded at 9,600 Hz. Based on experimental studies, authors extended ideal gas model application range to 1.5 bar_g.

KEYWORDS

gas explosion, propane, ideal gas model, model extension, closed vessel

1. INTRODUCTION

Dust and gas explosions or flame spread occur in everyday life [1] and a wide range in industrial segments from wood industry to food or chemical applications and mining. Dust safety science report of Cloney [2] summarized 28 dust explosions, 51 fire incidents and 8 fatalities worldwide, between January and June of 2021. Prevention of serious damages [3] based on four pillars: explosion-proof construction, avoidance of spread, suppression, and venting.

As it can be seen in Fig. 1, during explosion in closed vessels, the pressure rises quickly to maximum explosion overpressure (P_{max}), which can exceed maximum allowable pressure of the enclosure or the building. Besides the rate of pressure rise (dP/dt) is a significant value too, which is the slope of the inflection point of the pressure rise curve. These characteristics depend on the concentration of explosive material in fuel-air mixture between lower and upper explosibility limits. From the rate of pressure rise, a well-comparable deflagration index can be produced with the so-called cubic root law.

The maximum pressure values and deflagration indexes can be used to design proper venting protection for vessels and enclosures. Explosion venting devices, when pressure inside the vessel reaches their static activation pressure, become open in their full area and reduce the pressure inside the vessel, below the resistance of protected equipment, as it can be seen in Fig. 1.

Extensive experimental and theoretical studies are available to determine explosion characteristics in case of both unvented and vented cases; however their reliability varies according to scale of investigated chamber, and applied fuel. Some of the correlations have been included to international standards.

Explosion modeling work can be classified into three main categories:

- empirical correlations, such as model of Huzayyin et al. [4], or work of Razus et al. [5];
- phenomenological models, like Frolov model [6] or ideal gas model; and
- CFD models, like EXSIM code or FLACS. CFD models can give satisfactory accurate solution, however they are not led to the solution as fast as industrial calculations need.

*Corresponding author.
E-mail: viktoria.mikaczo@uni-miskolc.hu

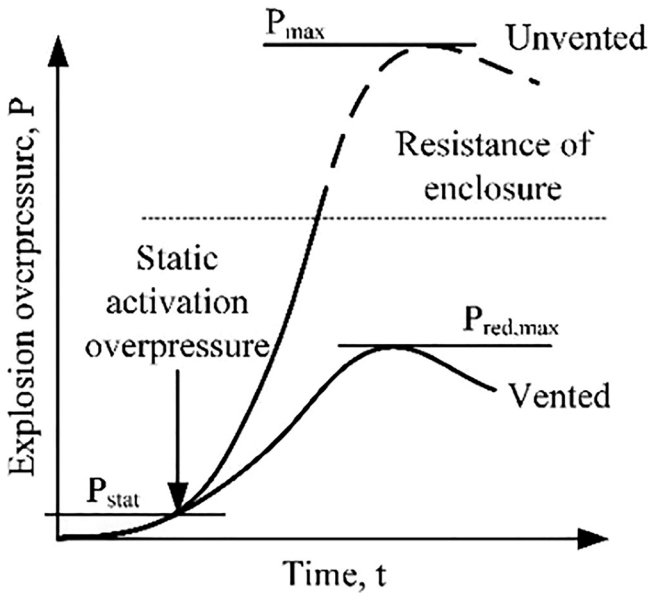

Fig. 1. Effect of venting protection to explosion pressure rise

On the contrary, the first two models give more simple correlations to predict explosion characteristics than the CFD models, they typically approach maximum rate of pressure rise and deflagration index. Mokhtar et al. [7] investigated the most widespread vented models against experimental studies. They found, e.g., in case of propane-air mixtures, that the errors of reduced explosion overpressures estimated according to EN 14994 standard [8], NFPA 68 standard [9], Bradley and Mitcheson method [10] and Molkov method [11] approximate to measurement results by a wide margin between 0.0068 and 52.258 relative error. Lautkaski [12] studied vented explosion models and vented ones with duct. Author revealed that in case of different fuels – natural gas, methane, and propane –similarly significant relative errors have been found against measured maximum explosion overpressures. Investigated correlations had been interpreted into NFPA 68 and VDI 3673 standards [9, 13].

It is clear, that most of the mathematical models, which are typically used to calculate vented explosions are very imprecise, but many of these equations have been incorporated into international standards of explosion protection.

To make applicable methods more precise besides keeping them as simple as possible, authors in this paper investigated propane deflagrations in closed vessel, since it is a widely used explosive gas in industrial processes. Authors carried out some experimental studies in a 20-L explosion sphere at ambient temperature and atmospheric initial pressure. Based on their experimental studies, they extended ideal gas model application range to 1.5 bar_g.

A further aim of their research is to develop such correlations for the maximum explosion pressure in case of vented and unvented explosions, for most common gas mixtures in industry, which can describe processes with more proper accuracy than currently used relationships.

2. IDEAL GAS MODEL

2.1. Original form of ideal gas model

Ideal gas model is one of the phenomenological models of gas explosion. The model assumes a fully premixed air-fuel mixture in a closed volume before combustion occurs. Ignition source assumed infinitesimally small with proper amount energy to start self-sustaining deflagration, and at significant distance from the walls.

In closed volumes, initial section of gas-air mixture deflagration can be assumed as burning of an ideal gas mixture. According to this model, the distribution of burnt and unburn phases, and the temperature and the pressure in the whole volume can be assumed fully homogenous, as the flame front passes through. Between them, the flame front thickness can be neglected according to the "thin flame model". In this case, ideal gas law can be written for both phases according to Eqs (1) and (2):

$$P \cdot V_u = \frac{m_u \cdot R_0 \cdot T_0}{M_u}, \tag{1}$$

$$P \cdot V_b = \frac{m_b \cdot R_0 \cdot T_b}{M_b}, \tag{2}$$

where m is the weight of the gas mixture in burnt and unburnt sections [kg], R_0 is universal gas constant [J $mol^{-1} \cdot K$], T is thermodynamic temperature [K], M is average molecular weight in each section [g mol^{-1}]. In the relations (1) and (2) and in the following, u refers to un-burnt, and b refers to burnt mixture, and 0 refers to initial state.

In the initial section of deflagration, flame is negligibly stretched, and no wrinkling is observed. These statements are valid up to maximum 10% of the pressure rise related to the initial pressure [14]. The change of the burnt material mass during explosion:

$$\frac{dm_b}{dt} = A_f \cdot \rho_u \cdot S_l, \tag{3}$$

where A_f is the area of flame front [m^2], ρ is the density of the mixture [kg m^{-3}] and S_l is the laminar burning velocity [m s^{-1}]. On the left side of Eq. (3), dm_b/dt can be separated to two parts: to flame velocity and burning velocity:

$$\rho_b \frac{dV_b}{dt} + V_b \frac{d\rho_b}{dt} = A_f \cdot \rho_u \cdot S_l, \tag{4}$$

Let r be the instantenous distance that the flame already travelled from the center of the explosion. In this case, momentary surface of the unwrinkled flame front can be interpreted as $dV_b/dr = A_f$. The flame velocity is $dr/dt = S_f$. Using Eq. (4), it can be written as:

$$S_f = \left(\frac{\rho_u}{\rho_b}\right) \cdot S_l - \left(\frac{V_b}{\rho_b \cdot A_f}\right)\left(\frac{d\rho_b}{dt}\right). \tag{5}$$

The surface of the flame in the direction of propagation is A_n, which is equal to the flow cross section. However, after the initial laminar propagation, flame become wrinkled, stretched, torn in some places, and real A_f flame surface is

higher than A_n. Because of the distortion of the flame front, modification of Eq. (5) is required. Since the change of density at the initial stage of the explosion is approximately zero, Eq. (5) can be simplified. In Eq. (5), $\rho_u/\rho_b = E$ is expansion factor. At the initial section of the flame propagation, T_b and T_u can be considered as constant values, so applying Eqs (1), (3) and (4), it can be written in simplified form:

$$V_t \cdot \frac{dP}{dt} = A_f \cdot S_l \cdot P \cdot (E-1). \tag{6}$$

At the initial stage of explosion, flame front expands without significant change in temperature to r_b radius, with temporarily negligible density change. Area of the flame front is:

$$A_f = 4\pi \cdot r_b^2 = 4\pi \cdot \left(S_f \cdot t\right)^2 = 4\pi \cdot (E \cdot S_l \cdot t)^2. \tag{7}$$

Using Eqs (6) and (7), Eq. (8) can be written as:

$$V_t \cdot \frac{dP}{dt} = P \cdot E^2 (E-1) \cdot S_l^3 \cdot 4\pi \cdot t^2, \tag{8}$$

and

$$\frac{1}{P}\frac{dP}{dt} = \frac{E^2(E-1) \cdot S_l^3 \cdot 4\pi \cdot t^2}{V_t}. \tag{9}$$

Integrating Eq. (9) from P_0 initial pressure to P it results, and regarding that investigated explosion chamber is a closed volume with radius R:

$$P = P_0 \cdot e^{E^2 \cdot (E-1)\left(\frac{S_l \cdot t}{R}\right)^3}. \tag{10}$$

2.2. Extended form of ideal gas model

From the conditions of ideal gas model can be seen, - as mentioned above - Eq. (10) only valid if the pressure is 10% above the initial pressure during explosion, i.e., approximately during laminar phase of the flame propagation [14]. Aim of this research was to establish the formal extension of the model up to 1.5 bar_g, in case of atmospheric initial state (to 150% above initial pressure).

The mathematical formula of Eq. (10) - due to its exponential form - could provide appropriate results up to the inflection point of measured pressure rise curves. Eq. (10) can be modified as the following:

$$P = P_0 \cdot e^{\varepsilon \cdot E^2 \cdot (E-1)\left(\frac{S_l \cdot t}{R}\right)^3}, \tag{11}$$

where ε is the factor that authors introduced to quantify the effect of the sub-progresses during turbulent flame propagation.

Expansion factor for propane-air mixtures was calculated by Brinzea et al. [9]. To facilitate further calculations, the function Eq. (12) was fitted to the original literature values. The coefficient of the determination of the function is $R^2 = 0.9817$,

$$E = 0.0795 \cdot V_{p,0}^3 - 1.4415 \cdot V_{p,0}^2 + 8.2717 \cdot V_{p,0} - 7.2286, \tag{12}$$

where $V_{p,0}$ is the initial propane volumetric concentration in the mixture. Estimation of E in polynomial form gives far more compact equation than calculating density of gas phase. In addition, the instantaneous density of the gas phase is significantly dependent on the momentary flame temperature, which is not the same as isobaric flame temperature, but is a function of heat loss.

Isobaric flame temperature was also determined by Brinzea et al. [7] as a function of propane content. To facilitate further calculations, the function Eq. (13) was fitted to the original literature values. The coefficient of determination of the function is $R^2 = 0.9869$,

$$T_{f,p} = 24.174 \cdot V_{p,0}^3 - 440.5 \cdot V_{p,0}^2 + 2446.3 \cdot V_{p,0} - 2066.1. \tag{13}$$

The S_l is the laminar burning velocity were determined according to measurement data in the following literature: Babkin (in Huzayyin et al. [4]), Liu [14], Brinzea [15]. Coefficient of determination of the approximation function Eq. (14) is $R^2 = 1$,

$$S_l = 0.0232 \cdot V_{p,0}^4 - 0.4247 \cdot V_{p,0}^3 + 2.7618 \cdot V_{p,0}^2 - 7.4914 \cdot V_{p,0} + 7.4164. \tag{14}$$

3. MEASUREMENTS

Some experimental studies were made with closed vessel to validate the extended model. Authors made the test sphere with propane-air mixtures at different concentrations between 2.8 and 6.3 vol%.

3.1. Experimental set-up

Main parts of Kühner test chamber were designed according to the principles of standard EN 14034-2:2006 +A1:2011 [16]. The test chamber is a 20-L hollow sphere with double stainless steel wall, which serves as water-cooled jacket to transfer the heat and to thermostatically control the test temperatures. The explosion pressure inside the vessel is recorded with three independent pressure transducers of 9,600 Hz. The process control and data acquisition unit operated on the computer with data collection function.

Propane-air mixtures with 2.8–6.3 vol% were used in experiments. Air was applied from the environment for more realistic measurements. For testing, the gas in proper concentration is dispersed into the vacuumed chamber via gas filling nozzle. The ignition source is located in the center of the sphere. For gases, it is an electric spark, with computer-regulated 10 J energy.

3.2. Experimental process

Experimental studies were performed at atmospheric pressure (1 bar_g) and ambient temperature (298 K). To increase

the reliability of the measurements, a filling chamber was designed and produced with 0.6 L volume, including all fittings. Its function was to fill the required amount of propane to the 20-L chamber. The desired propane amount was checked by a pressure transducer placed in the filling chamber, also at a frequency of 9,600 Hz.

Scheme of complete measurement setup with the gas filling chamber is shown in Fig. 2. At the Fig. 1 means gas filling chamber, *2* means Kühner explosion chamber. *P*1 shows pressure transducer connected to the filling chamber and *P*2 shows pressure transducer connected to explosion chamber. Both were P6A type, made by Hottinger Brüel & Kjaer GmbH. The chamber originally is equipped with, and ignition process was controlled automatically by *K*1 and *K*2 are Kistler piezoelectric pressure transducers.

The different stages of the closed chamber measurements are illustrated in Fig. 3. Solid line shows the characteristic curve of the pressure values recorded in the 20-L chamber, while the dashed line shows the characteristic curve of the pressure values recorded in the filling chamber.

In stage 1, the filling chamber and the explosion chamber were simultaneously vacuumed to a predefined value. At the end of vacuuming, the connection between the two chambers was eliminated by closing the ball valve between them.

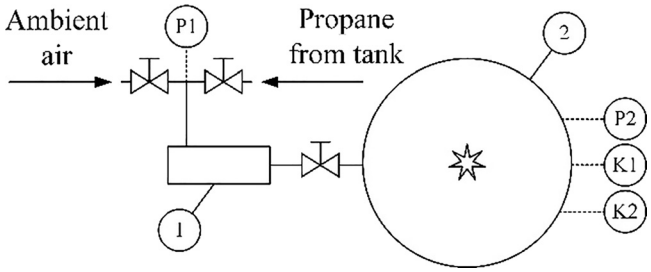

Fig. 2. Scheme of experimental setup

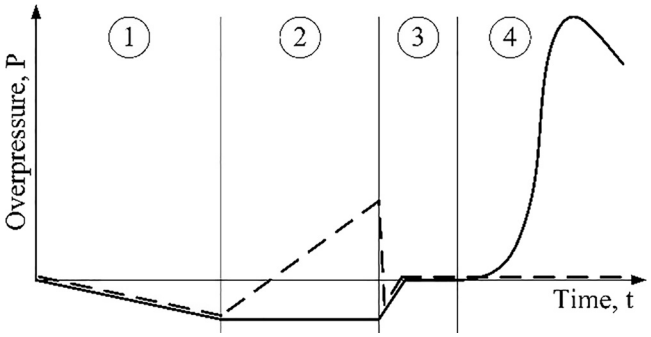

Fig. 3. Stages of measurements

In stage 2, propane was loaded into the filling chamber, also up to a predetermined overpressure, in order to reach the proper amount in the mixture. Proper loading pressures of propane determine the composition of explosive mixture in the chamber.

After propane loading, the ball valve between the two chambers was opened again, and part of the propane gas flowed into the explosion chamber in stage 3. At the end of this process, small amount of propane remains in the filling chamber, and the pressure is slightly less than ambient pressure. In order to eliminate the vacuum and flush the filling chamber, the missing air volume was provided from the ambient air by passing it through the filling chamber. At the end of the section, all openings on the explosion chamber were closed. . The filling method of the chamber and the resulting high degree of turbulence provides homogenous gas mixture in the chamber.

In stage 4, ignition was performed after a software-controlled delay of 60 ms, which ensures dissipation of turbulence before ignition, however gas components do not separate at this time. Pressure values in the chamber during the explosion were recorded. After the explosion occurred, the whole system was thoroughly ventilated to remove residual gases and combustion products.

3.3. Measurement results

As mentioned before, the tests were performed with propane-air mixture. The compositions of the mixtures were 2.8, 3.8, 4.8, 5.8 and 6.3 vol% propane in air. Typical explosion values (maximum explosion overpressure and deflagration index) from the tests are summarized in Table 1. For each concentration, at least five different measurements were developed, discarding the smallest and largest of these, and averaging the others. Furthermore, as it can be seen from the description of the measurement, the pressure values in the explosion chamber were recorded by three independent pressure transmitters, so that the characteristic values for a single concentration is the average of at least nine different measurements.

The averages of measured maximum explosion pressure values compared to the literature data (Razus et al. [5], NFPA 68 [9], Cashdollar et al. [17]) are illustrated in Fig. 4. The measured values correlate with the literature, with an average deviation under 3.5% (see Table 1).

Table 1. Measured explosion characteristics

Propane amount [vol%]	Maximum explosion overpressure P_{max} [bar_g]	Deviation of measured P_{max} values	Deflagration index K_G [bar·m s^{-1}]	Deviation of measured K_G values
2.8	5.46	+1.4%, −2.18%	21	+3.04%, −6.08%
3.8	7.36	+1.72%, +0.04%	85	+8.59%, −6.05%
4.8	7.91	+1.46%, −2.54%	111	+1.38%, −2.27%
5.8	7.15	+1.21%, −1.26%	49	+8.44%, −9.17%
6.3	6.54	+3.44%, −2.46%	23	+22.83%, −18.50%

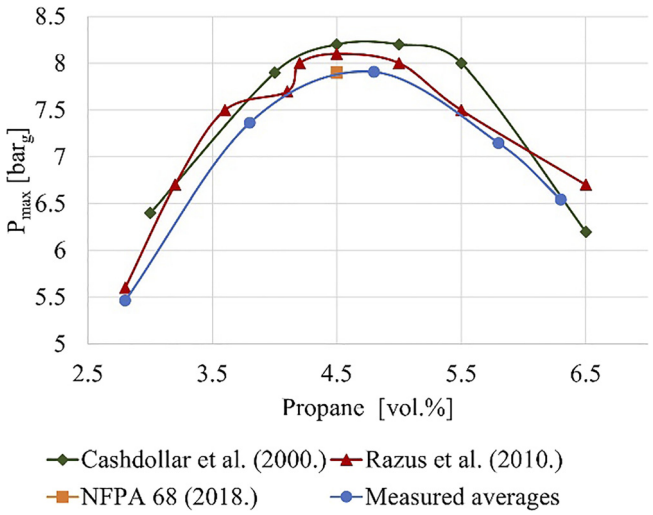

Fig. 4. Maximum explosion overpressures

The measured deflagration indexes were compared the literature data (Huzayyin et al. [4]) is illustrated in Fig. 5. Since the initial turbulence has an extreme influence on the instantaneous flame velocity and on the rate of explosion pressure rise, this may explain significant deviation in measured values (see Table 1) and high discrepancy with the literature - although any information in the source cannot be found.

Based on literature and measured data of maximum explosion overpressure, and rate of pressure rise, extended ideal gas model can be established.

4. EXTENSION OF IDEAL GAS MODEL

Original ideal gas model was adequate until the pressure rise reaches maximum 10% above to initial absolute pressure. However, most of the explosion venting devices opens when the pressure is 10% above of operating pressure. Therefore, extension of ideal gas model was carried

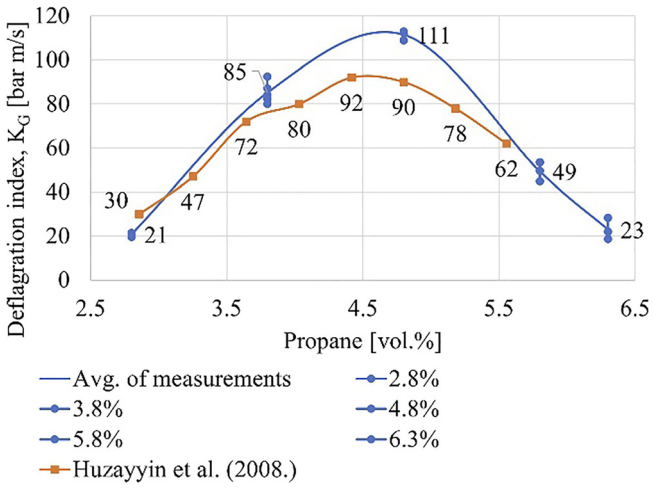

Fig. 5. Deflagration indexes

to 150% above the initial atmospheric pressure to cover activation pressures of venting devices, too. To extend the model, authors defined an ε factor in the original model and determined its values in the function of propane concentration. To determine ε factor in Eq. (11), authors fitted them to the real measurement results as a function of initial propane amount in the mixture. The sum of squared errors of the fitted function was within 0.6 bar^2 in all cases.

The values of ε correction factor obtained by this method are illustrated in Fig. 6.

As it can be seen in Fig. 6, the factor is strongly dependent on the propane concentration, and the function relationship can be described by a second order function. Approximation function is marked with stipple in Fig. 6, and equation of the fitted function is the following:

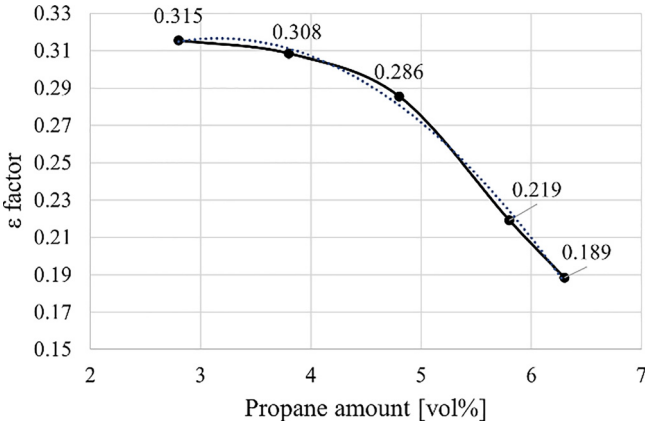

Fig. 6. Values of ε correction factor related to propane amount

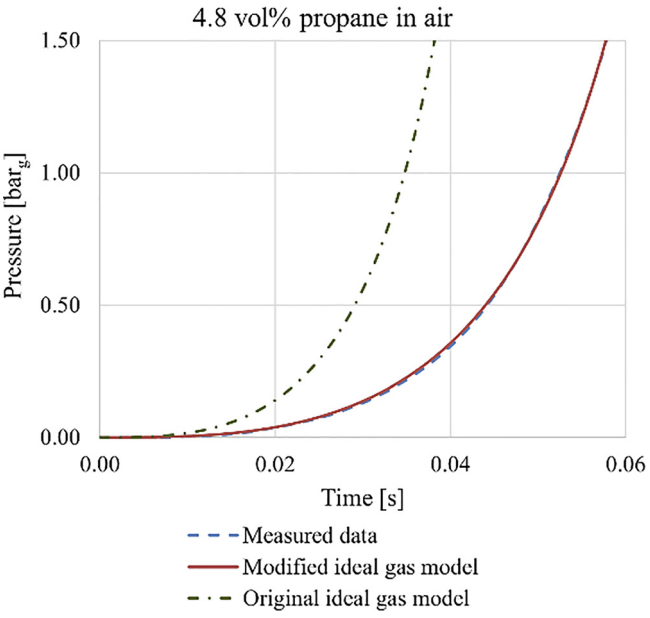

Fig. 7. Measured and modeled pressure values according to original and modified ideal gas model, in case of 4.8 vol% propane-air mixture

$$\varepsilon = -0.0132 \cdot V_{p,0}^2 + 0.0832 \cdot V_{p,0} + 0.1853. \qquad (15)$$

Coefficient in the approximation function, Eq. (12) is $R^2 = 0.9952$. As it can be seen in Fig. 7, the original form of the model cannot reproduce measured pressure values in wide pressure range, along with different initial gas compositions. The figure shows three examples for modeled pressure rise according to original ideal gas model by Eq. (10), and modified ideal gas model by Eqs (11) and (15), compared to measured data by authors. Figure 7 illustrates the middle of the investigated mixture domain (4.8 vol%).

5. CONCLUSIONS

In this research, authors studied ideal gas model for 20-L volume closed vessel. They developed new, more accurate gas filling system for test chamber, and carried out closed vessel explosion measurements in wide range of propane amount. Based on these experiments, authors extended ideal gas model to wider range of explosion pressure rise.

Application range of former ideal gas model were extended from $1.1P_0$ to $2.5P_0$ when P_0 equals to atmospheric pressure and initial temperature is 298 K. The form of extension is applicable when explosive atmosphere is propane-air mixture and its propane content is between 2.8 vol% and 6.3 vol%.

These studies can be used to predict explosion pressure values inside closed vessel related to time and initial propane content. Development of the new model will be continued with vented explosion cases and developing a vented model for propane explosions.

REFERENCES

[1] G. László, F. Hajdu, and R. Kuti, "Experimental study on examining the fire load of a small compartment," *Pollack Period.*, vol. 17, no. 1, pp. 133–138, 2022.

[2] Dust Safety Science, Combustible Dust Incident Report Summary, 2021. [Online]. Available: https://dustsafetyscience.com/2021-report-summary/. Accessed: Jan. 10, 2022.

[3] S. Nemer and F. Papp, "Influence of imperfections in the buckling resistance of steel beam-columns under fire," *Pollack Period.*, vol. 16, no. 3, pp. 1–6, 2021.

[4] A. S. Huzayyin, H. A. Moneib, M. S. Shehatta, and A. M. A. Attia, "Laminar burning velocity and explosion index of LPG-air and propane-air mixtures," *Fuel*, vol. 87, no. 1, pp. 39–57, 2008.

[5] D. Razus, V. Brinzea, M. Mitu, and D. Oancea, "Temperature and pressure influence on explosion pressure of closed vessel propane-air deflagrations," *J. Hazard. Mater.*, vol. 174, nos 1–3, pp. 548–555, 2010.

[6] S. M. Frolov, V. S. Aksenov, and I. O. Shamshin, "Reactive shock and detonation propagation in U-bend tubes," *J. Loss Prev. Process Ind.*, vol. 20, nos 4–6, pp. 501–508, 2007.

[7] K. M. Mokhtar, R. M. Kasmani, C. R. C. Hassan, M. D. Hamid, S. D. Emami, and M. I. M. Nor, "Reliability and applicability of empirical equation in predicting the reduced explosion pressure of vented gas explosion," *J. Loss Prev. Process Ind.*, vol. 63, 2020, Paper no. 104023.

[8] *EN 14491:2012*, Dust explosion venting protective systems, CEN, Brussels, 2012.

[9] *NFPA 68*, Standard on explosion protection by deflagration venting, national fire protection association, Quincy, Massachusetts, 2018.

[10] D. Bradley and A. Mitcheson, "The venting of gaseous explosions in spherical vessels II – theory and experiment," *Combustion and Flame*, vol. 32, pp. 237–255, 1987.

[11] V. V. Molkov, A. Korolchenko, and S. Aksenov, "Venting of deflagrations in buildings and equipment: Universal correlation," *Fire Saf. Sci.*, vol. 5, pp. 1249–1260, 1997.

[12] R. Lautkaski, "Duct venting of gas explosions, Revision of two proposed engineering correlations," *J. Loss Prev. Process Ind.*, vol. 25, pp. 400–413, 2012.

[13] *VDI 3673 Blatt 1*, Pressure venting of dust explosions, Düsseldorf, 2002.

[14] Q. Liu, Y. Zhang, F. Niu, and L. Li, "Study on the flame propagation and gas explosion in propane/air mixtures," *Fuel*, vol. 140, pp. 677–684, 2015.

[15] V. Brinzea, M. Mitu, C. Movileanu, A. Musuc, D. Razus, and D. Oancea, "Propagation velocities of propane-air deflagrations at normal and elevated pressures and temperatures," *Revista de Chim.*, vol. 63, no. 3, pp. 289–292, 2012.

[16] *EN 14034-2:2006+A1:2011*, Determination of explosion characteristics of dust clouds. Part 2: Determination of the maximum rate of explosion pressure rise (dp/dt) max of dust clouds, CEN, Bruxelles, 2006.

[17] K. L. Cashdollar, "Overview of dust explosibility characteristics," *J. Loss Prev. Process Ind.*, vol. 13, nos 3–5, pp. 183–199, 2000.